INTERNATIONAL TABLES FOR CRYSTALLOGRAPHY

ISSN 1574-8707
it.iucr.org

Volume I, X-ray Absorption Spectroscopy and Related Techniques
ISBN: 978-1-119-43394-1

Chapter 5.10

Received 27 October 2016
Accepted 2 July 2020

Keywords: theoretical calculations; phase shifts; amplitudes.

Related chapters

Volume I: 2.1, 2.13, 2.14, 2.25, 3.43, 4.6, 4.7, 5.2, 5.4, 5.6, 5.7, 5.9

Importance of theoretical calculations for phase shifts and amplitudes

Matthew Newville[a]* and Bruce Ravel[b]

[a]Center for Advanced Radiation Sources, The University of Chicago, Chicago, IL 60637, USA, and [b]National Institute of Standards and Technology, Gaithersburg, MD 20899, USA. *Correspondence e-mail: newville@cars.uchicago.edu

In order to model experimental extended X-ray absorption fine-structure (EXAFS) data to extract quantitative structural parameters N, R and σ^2 for the neighboring atoms, accurate functions for the photoelectron scattering phase shifts and amplitudes are required. These depend strongly on the photoelectron wavenumber k and on the species (Z) of the absorbing and scattering atom, and to a somewhat lesser degree on the distance R to the neighboring atom. While scattering factors can be derived from experimental data in certain limited cases, the use of *ab initio* theoretical scattering phase shifts and amplitudes has greatly expanded the ability to model more complex structures and to include the effects of multiple scattering. While the calculations are complex and the results of these calculations still cannot match the accuracy of high-quality experimental EXAFS measurements, they have been demonstrated to accurately model EXAFS in a great number of systems over the past 30 years. Here, some of the finer points of the uses and limitations of applying theoretical scattering factors to the analysis of experimental EXAFS spectra are discussed.

1. Scattering factors for EXAFS analysis

Quantitative modeling of EXAFS requires accurate values for the photoelectron scattering amplitudes and phase shifts in order to determine the structural parameters for the neighbor atoms. A simple form of the EXAFS equation is

$$\chi(k) = \sum_j \frac{N_j f_j(k) \exp[-2R_j/\lambda(k)] \exp(-2k^2\sigma_j^2)}{kR_j^2} \times \sin[2kR_j + \delta_j(k)], \qquad (1)$$

where the summation is over scattering paths j of the emitted photoelectron. The scattering amplitude $f(k)$ and phase shift $\delta(k)$ are required for each path in order to extract the structural parameters the coordination number N, the neighbor distance R and the mean-square displacement in the neighbor distance σ^2. The photoelectron mean free path $\lambda(k)$ is also required, although this is expected to have a near-universal dependence on photoelectron wavenumber (Seah & Dench, 1979). Fig. 1 shows $\lambda(k)$, which varies between 5 and 50 Å over the typical EXAFS range, and the variations observed in calculations using *FEFF* (Rehr *et al.*, 1991; Kas *et al.*, 2024) of $\lambda(k)$ for different backscattering atoms.

The factors $f(k)$ and $\delta(k)$ represent the scattering of a photoelectron from surrounding atoms with a kinetic energy of a few hundred electronvolts. In a condensed-matter system these scattering factors are nontrivial quantities that depend strongly on k and on the Z of the scattering atom. Fig. 2 shows $f(k)$ for a few scattering atoms (oxygen, iron and lead) and Fig. 3 shows $\delta(k)$ for the same scattering atoms. As more scattering paths and especially multiple-scattering paths are added, the interdependence of the scattering terms with the structural parameters becomes very complicated. Thus, it was recognized very early on (Lee & Pendry, 1975) in the modern EXAFS era (Sayers *et al.*, 1971) that accurate calculations of these 'ghosts of 'lectricity' (Dylan, 1966) were necessary in order to be able to use EXAFS for quantitative characterization of local atomic structure.

2. The development of theoretical phase shifts and amplitudes

Many early attempts were made to use theoretical calculations of EXAFS scattering factors for quantitative analysis, but the relatively poor agreement between early theoretical calculations and experimental measurements meant that much of the work published prior to 1985 did not use *ab initio* calculations. Even as the calculations became more reliable, the relative expense of the computations led to the tabulation (McKale *et al.*, 1988) of representative calculations that were used for the quantitative analysis of many experimental spectra well into the 1990s.

Between 1975 and 1995, considerable effort was made to develop accurate and efficient *ab initio* calculations of the photoelectron scattering factors for EXAFS. While Rehr & Albers (2000) give a more detailed history, and explore the complexities involved in accurately and efficiently accounting for many-body effects and multiple scattering, here we mention the principal concepts and theoretical developments needed for accurate EXAFS calculations. These include consideration of the overlapped atomic potentials for a solid in the excited state, typically using a 'muffin-tin approximation' for the electron density and an unrelaxed '$Z + 1$ approximation' for the electronic state of the absorbing atom, including relativistic effects for heavy elements as appropriate. It has also been shown that curved-wave effects (Müller & Schaich, 1983; Gurman *et al.*, 1984) in the photoelectron scattering are important for accurate calculation of the scattering factors. In addition to including extrinsic losses as described by a mean free path for the photoelectron, considerable effort (Mustre de Leon *et al.*, 1991) has gone into accounting for the self-energy due to exchange interactions and many-electron effects in the excited state (Hedin & Lundqvist, 1971), as well as accounting for intrinsic losses due to the response to the core hole. Finally, the efficient calculation of multiple scattering of the photoelectron (Rehr & Albers, 1990) has been critical in the ability to fully account for many EXAFS spectra beyond the first shell.

By the late 1980s and early 1990s these efforts led to calculations that were accurate enough for the reliable analysis of experimental EXAFS spectra (Mustre de Leon *et al.*, 1991). Subsequent developments included efficient and accurate multiple-scattering contributions (Zabinsky *et al.*, 1995), allowing the form of equation (1) to be used for

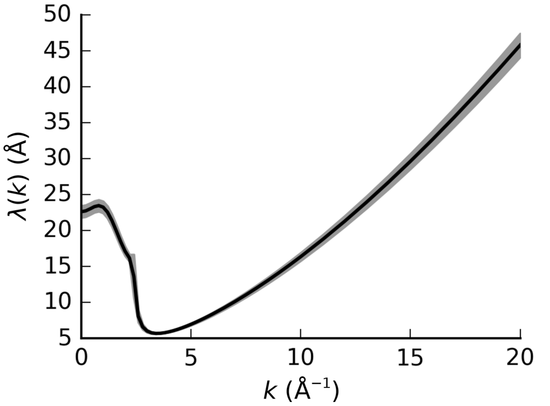

Figure 1
The k dependence of the photoelectron mean free path $\lambda(k)$. The curve is generally considered to be 'universal' in that it is largely independent of material. The gray area shows the typical variation seen for calculations of $\lambda(k)$ for the same absorbing atom and neighbor distance, but with neighbors with a wide range of Z. The finite mean free path is one of the principal reasons that EXAFS is inherently sensitive only to short-range order.

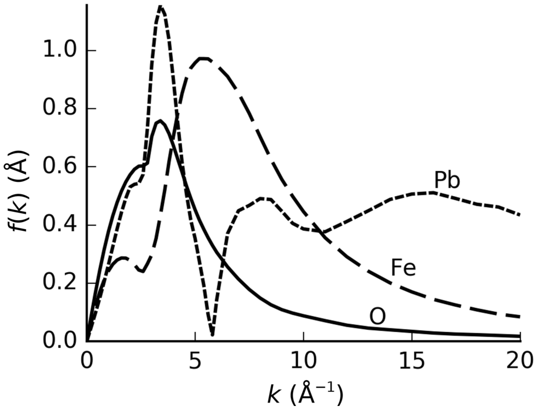

Figure 2
The k dependence of the photoelectron scattering amplitude $f(k)$ for oxygen (solid lines), iron (long dashed lines) and lead (short dashed lines). The strong k dependence shows that heavier elements tend to be stronger scatterers especially at high k and that sharp resonances can be appreciable for high-Z atoms. This strong Z dependence gives EXAFS sensitivity to the species of the scattering atoms as well as their distance R and coordination number N.

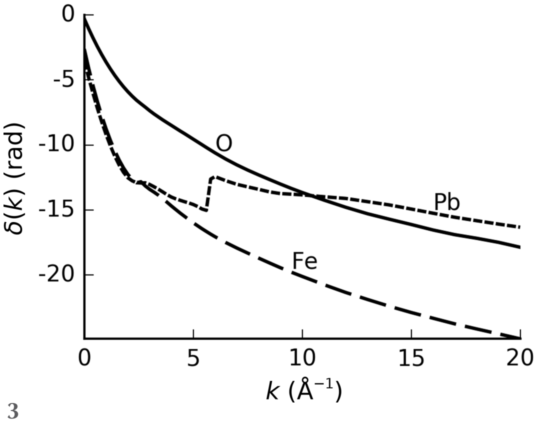

Figure 3
The k dependence of the photoelectron scattering phase shift $\delta(k)$ for oxygen (solid lines), iron (long dashed lines) and lead (short dashed lines). As with $f(k)$, the strong Z dependence gives EXAFS sensitivity to the species of the scattering atom. The general negative slope of $\delta(k)$ shifts peaks in Fourier-transformed EXAFS to R below the near-neighbor distance.

multiple-scattering as well as single-scattering paths, and the full inclusion of polarization dependence (Ankudinov & Rehr, 1997) for anisotropic structures and magnetic systems. While two computer codes, *EXCURVE* (Binsted & Hasnain, 1996; Feiters *et al.*, 2024) and *GNXAS* (Filipponi *et al.*, 1995; Filipponi, Di Cicco *et al.*, 2024; Filipponi, Natoli *et al.*, 2024), used such calculations within a complete analysis framework for EXAFS modeling and analysis, many separate analysis codes (Stern *et al.*, 1995; George & Pickering, 2000; Ressler, 1998; Newville, 2001) were built on top of the *FEFF* code (Rehr *et al.*, 1991; Zabinsky *et al.*, 1995; Kas *et al.*, 2024) which allowed EXAFS spectra to be modeled with very high accuracy for a wide range of systems (O'Day *et al.*, 1994; Vaarkamp *et al.*, 1994). During this time there was considerable development of both the theoretical and the analytical computer code, with sharing of ideas between them. After the passing of several decades, nearly all published EXAFS analyses now use theoretical phase shifts and amplitudes from *FEFF* or similar programs.

3. Limits of empirical phase shifts and amplitudes

Prior to accurate *ab initio* calculations becoming readily available, many analyses tried to extract scattering factors (phase shifts and amplitudes) from experimentally measured EXAFS spectra of samples with well known structures. Producing such *empirical standards* requires isolating a single EXAFS 'shell' by Fourier filtering so that the dominant $2kR$ term of the phase can be removed. Accurate extraction of these terms is limited to surprisingly few structures, as there is no reliable mechanism to extract measurement uncertainties for empirical standards when they are affected by mixtures of shells or leakage of multiple-scattering paths, both of which are common in all but the simplest crystal structures. The extraction of empirical standards is particularly difficult for highly disordered systems such as glasses or disordered, multisite crystal structures with a wide range of distances in the first shell. In some cases, hybrid solutions that combine empirical scattering factors extracted from well characterized materials with differences of theoretical or tabulated scattering factors can be used. These approaches are somewhat involved, but can give scattering factors for pairs of atoms for which simple standard materials were not available. While many analyses of EXAFS data using such empirical or semi-empirical standards have given reliable and accurate results, these analyses essentially all ignore of the contributions of multiple scattering and so are best used for first-neighbor shells, where these effects are usually negligible.

Still, it must be acknowledged that for investigating *relative* changes in simple structures, differential analyses that effectively cancel the importance of the scattering factors can be more precise than analyses that use calculated values of $f(k)$ and $\delta(k)$ in order to fully model and absolutely determine R and N from EXAFS spectra. For example, in investigating the temperature dependence of a near-neighbor atom at low-to-modest disorder, using a differential analysis without theoretical scattering factors can give extremely accurate changes in bond distances, whereas an analysis using *ab initio* calculations may be dominated by the absolute differences between the calculated and experimental spectra. To illustrate this point, Pettifer *et al.* (2005) were able to see changes in bond lengths of 10 fm in an iron–cobalt thin film from EXAFS data, a level of precision 100 times smaller than the typical uncertainties in absolute distances determined by EXAFS analysis. In this analysis, an extremely precise and stable measure of X-ray energy was necessary in addition to the use of a differential analysis of the EXAFS spectra, rather than an analysis which fully modeled the EXAFS oscillations.

4. Advantages of theoretical phase shifts and amplitudes

Using first-principles calculations to model EXAFS data with the EXAFS equation (1) allows a few important conveniences that greatly expand the applicability of EXAFS analysis. One such convenience is that the calculations can easily account for the polarization dependence of EXAFS, which is tedious to perform with empirical standards. In addition to avoiding the limitations of empirical standards described above, one can use theoretical scattering factors to readily predict EXAFS spectra for arbitrarily complex structures.

Because the theoretical calculations properly combine all of the inelastic loss terms (including the mean free path and self-energies from the exchange terms), the photoelectron wavenumber k can be replaced with its complex value extension $p = k + i/\lambda(k)$, that is with $1/\lambda(k)$ giving the imaginary part of the wavenumber. With this extension, equation (1) becomes

$$\chi(k) = \sum_j \operatorname{Im}\left\{\frac{N_j f_j(k)\exp[2ipR_j + i\delta_j(k)]\exp(-2p^2\sigma_j^2)}{pR_j^2}\right\}, \quad (2)$$

where k is now replaced by p throughout, with the value of k used only to index the values of f and δ, and the imaginary part of the complex quantity is taken to give the sine-like function.

Using the complex wavenumber better accounts for the effect of disorder terms such as σ^2 and higher cumulants (Bunker, 1983) that are not explicitly shown in equation (2). That is, a distribution of distances R represented by a mean R and σ^2 causes not only a k^2-dependent reduction in the EXAFS amplitude but also a modest phase shift that might otherwise be assigned to a change in mean distance. Although a minor point for small disorder, these effects can be noticeable as structural disorder increases and can be readily accommodated when using theoretical scattering factors.

When using theoretical scattering terms, the sum does not need to be over well isolated shells, but can include shells of mixed species and overlapping shells with many individual contributions over a finite range of distances. For highly disordered systems, this allows EXAFS to be modeled in a few different ways. For example, the *GNXAS* approach (Filipponi *et al.*, 1995) integrates over the EXAFS equation using a parameterized radial distribution function based on the log-gamma distribution function. This can be performed either as a continuous integral or as a discretized sum with an resolution R that is much finer than required by the intrinsic resolution of the data (which is typically larger than 0.05 Å). Such approaches to modeling disorder can also readily include the effect from the $1/R^2$ term in the EXAFS equation, which is often left out of a cumulant expansion or accounted for with a correction factor. Alternatively, one can use an arbitrarily large cluster of atoms as from molecular-dynamics simulations or density-functional theory calculations to simulate the EXAFS with very many paths and then use reverse Monte Carlo approaches (Gurman & McGreevy, 1990) to select the most likely candidate structure.

The most important advantage of using theoretical scattering factors is that contributions from multiple-scattering paths can be accommodated seamlessly in the analysis when theoretical scattering factors are used, whereas they are extremely difficult to model with empirical scattering factors. It has long been recognized (Lee & Pendry, 1975) that certain multiple-scattering paths, most notably the ‘focused multiple-scattering paths’, as illustrated in Fig. 4, can have very large scattering amplitudes that depend strongly on bond angles. The availability of theoretical calculations that include multiple-scattering contributions allows these contributions to not only be taken into account but also exploited. For example, the strong angular dependence of the scattering amplitude for paths that are nearly collinear can be used to determine average bond angles in distorted structures (Frenkel *et al.*, 1994).

Contributions of multiple-scattering paths can also be important for quantitative analysis of first and second shells of EXAFS spectra. The phase shift shown in Fig. 3 for single-scattering paths can be seen to have a slope of approximately -1 rad Å^{-1}, which gives rise to a shift of roughly -0.5 Å to the Fourier-transformed EXAFS. This phase shift includes contributions from both absorbing and scattering atoms, so that multiple-scattering paths will generally have a somewhat larger and less linear shift, which both spreads out the contributions of these paths and shifts them to lower R. Thus, it is not uncommon for triangular paths between first and second neighbors to overlap strongly in R with second-shell EXAFS. While second-shell species can be identified and distances can be refined without considering multiple scattering for a few open structures, it is more often the case that including multiple-scattering contributions from theoretical calculations is necessary to accurately model second and further shells.

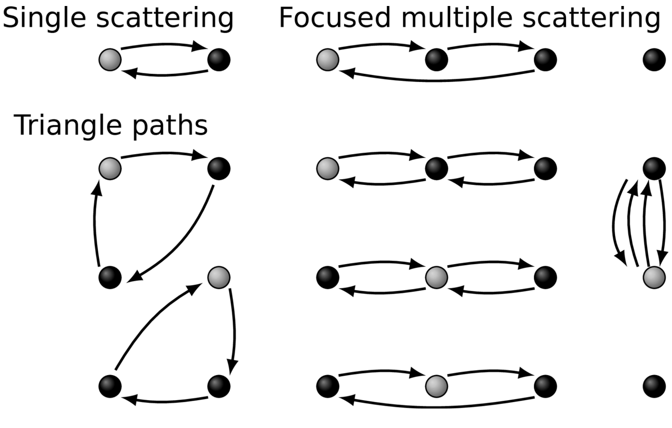

Figure 4
Examples of important multiple-scattering paths within a plane. Triangular paths have low, diffuse scattering amplitude in k and R, but there are many of them. Paths that involve multiple atoms and scattering angles near 180°, the so-called focused multiple-scattering paths, can have a very high amplitude that is strongly dependent on angle.

The need for calculation of the complex photoelectron scattering factors was recognized to be crucial for accurate modeling of EXAFS very early after the pioneering work of Sayers, Lytle and Stern (Sayers *et al.*, 1971). Considerable theoretical effort by a few dedicated groups over a few decades was required to realize general-purpose tools for *ab initio* calculations with accuracies comparable to experimental data. Once these theoretical tools became reliable and readily available, advances in analysis tools soon followed and the use of EXAFS for samples of increasing complexity has continued ever since. The improvements made in theoretical scattering factors and inelastic losses for EXAFS also enabled advances in the modeling of X-ray absorption near-edge spectroscopy, electron energy-loss spectroscopy, X-ray magnetic circular dichroism, diffraction anomalous fine structure, resonant and nonresonant inelastic X-ray scattering and other advanced X-ray and electron spectroscopies.

References

Ankudinov, A. & Rehr, J. (1997). *Phys. Rev. B*, **56**, R1712–R1716.
Binsted, N. & Hasnain, S. S. (1996). *J. Synchrotron Rad.* **3**, 185–196.
Bunker, G. (1983). *Nucl. Instrum. Methods Phys. Res.* **207**, 437–444.
Dylan, B. (1966). *Visions of Johanna*. Dwarf Music.
Feiters, M. C., Strange, R. W. & Binsted, N. (2024). *Int. Tables Crystallogr. I*, ch. 6.5, 744–751.
Filipponi, A., Di Cicco, A. & Natoli, C. R. (1995). *Phys. Rev. B*, **52**, 15122–15134.
Filipponi, A., Di Cicco, A & Natoli, C. R. (2024). *Int. Tables Crystallogr. I*, ch. 6.12, 787–790.
Filipponi, A., Natoli, C. R. & Di Cicco, A. (2024). *Int. Tables Crystallogr. I*, ch. 6.11, 782–786.
Frenkel, A., Stern, E. A., Voronel, A., Qian, M. & Newville, M. (1994). *Phys. Rev. B*, **49**, 11662–11674.
George, G. N. & Pickering, I. J. (2000). *EXAFSPAK: A Suite of Computer Programs for Analysis of X-ray Absorption Spectra*. https://www-ssrl.slac.stanford.edu/~george/exafspak/manual.pdf.
Gurman, S. J. & McGreevy, R. L. (1990). *J. Phys. Condens. Matter*, **2**, 9463–9473.
Gurman, S., Binsted, N. & Ross, I. (1984). *J. Phys. C Solid State Phys.* **17**, 143–151.
Hedin, L. & Lundqvist, B. I. (1971). *J. Phys. C Solid State Phys.* **4**, 2064–2083.
Kas, J. J., Vila, F. D. & Rehr, J. J. (2024). *Int. Tables Crystallogr. I*, ch. 6.8, 764–769.
Lee, P. A. & Pendry, J. B. (1975). *Phys. Rev. B*, **11**, 2795–2811.
McKale, A. G., Veal, B. W., Paulikas, A. P., Chan, S. K. & Knapp, G. S. (1988). *J. Am. Chem. Soc.* **110**, 3763–3768.
Müller, J. E. & Schaich, W. L. (1983). *Phys. Rev. B*, **27**, 6489–6492.
Mustre de Leon, J., Rehr, J. J., Zabinsky, S. I. & Albers, R. C. (1991). *Phys. Rev. B*, **44**, 4146–4156.
Newville, M. (2001). *J. Synchrotron Rad.* **8**, 322–324.
O’Day, P. A., Rehr, J. J., Zabinsky, S. I. & Brown, G. (1994). *J. Am. Chem. Soc.* **116**, 2938–2949.
Pettifer, R., Mathon, O., Pascarelli, S., Cooke, M. & Gibbs, M. (2005). *Nature*, **435**, 78–81.

Rehr, J. J. & Albers, R. C. (1990). *Phys. Rev. B*, **41**, 8139–8149.

Rehr, J. J. & Albers, R. C. (2000). *Rev. Mod. Phys.* **72**, 621–654.

Rehr, J. J., Mustre de Leon, J., Zabinsky, S. I. & Albers, R. C. (1991). *J. Am. Chem. Soc.* **113**, 5135–5140.

Ressler, T. (1998). *J. Synchrotron Rad.* **5**, 118–122.

Sayers, D. E., Stern, E. A. & Lytle, F. W. (1971). *Phys. Rev. Lett.* **27**, 1204–1207.

Seah, M. P. & Dench, W. A. (1979). *Surf. Interface Anal.* **1**, 2–11.

Stern, E. A., Newville, M., Ravel, B., Yacoby, Y. & Haskel, D. (1995). *Physica B*, **208–209**, 117–120.

Vaarkamp, M., Dring, I., Oldman, R. J., Stern, E. A. & Koningsberger, D. C. (1994). *Phys. Rev. B*, **50**, 7872–7883.

Zabinsky, S. I., Rehr, J. J., Ankudinov, A., Albers, R. C. & Eller, M. J. (1995). *Phys. Rev. B*, **52**, 2995–3009.